Anomalous elastic properties and bcc-fcc transition of cesium at high pressures up to 2.5 GPa

F. F. Voronov, O. V. Stal'gorova, and E. L. Gromnitskaya

L. F. Vereshchagin Institute of High Pressure Physics, Russian Academy of Sciences, 142092 Troitsk, Moscow Oblast, Russia

The propagation velocities of longitudinal and transverse ultrasonic waves have been measured in polycrystalline Cs at a temperature of 294 K and at pressures up to 2.5 GPa. The compression of Cs and all its elastic characteristics were found as a function of the pressure. There are anomalies on the plots of the bulk modulus, the shear modulus, and their derivatives versus the pressure and on the plot of the lattice constant versus the compression at $p > 1.4$ GPa. These anomalies point to a change in the *s–d* nature of the Cs conduction electrons. They support some existing theoretical predictions. The changes in the elastic properties of Cs at the bcc–fcc phase transition were determined. A soft shear mode appears in the cesium phonon spectrum in the pretransition region.

1. INTRODUCTION

The compression of cesium at high pressures causes a substantial decrease in volume ($\sim 50\%$ at 5 GPa) and gives rise to several interesting and clearly expressed effects which are associated with changes in the crystal structure and electronic structure of this material. The regions in which various phases of Cs exist on the phase diagram have been determined: At 295 K, bcc CsI exists from 0 to 2.3 GPa; fcc CsII exists from 2.3 to 4.3 GPa; the denser, isomorphic fcc CsII phase exists from 4.30 to 4.35 GPa; and tetragonal CsIV exists up to 10 GPa (Refs. 1 and 2). The melting curve has two peaks, at 2.0 GPa, 573 K and 3.0 GPa, 571 K. In the region in which the melting temperature decreases with the pressure, $p > 2.0$ GPa and $p > 3.0$ GPa, we would expect anomalies in the physical properties.

Pseudopotential calculations on the electronic spectrum of Cs show that compression of Cs may cause a continuous *s–d* transition, which would begin at a low pressure or at $p = 0$. This transition would occur in an avalanche fashion at 4–5 GPa and would not yet be terminated at 10 GPa (Refs. 3–6). It has been shown that there is a relationship between the electronic structure and the stability of the high-pressure phases. It has been asserted in particular that the bcc–fcc transition of Cs at 2.3 GPa is determined by the population of the *d* level (by the extent of the *s–d* transition)[7] and that ion–ion repulsion[8] plays a smaller role. Optical studies[9] of Cs have shown that a pronounced increase in absorption occurs for wavelengths below 3 eV at pressures of 0–1.8 GPa. This increase is directly associated with a change in the *d* nature of the conduction electrons. It has been suggested that the bcc–fcc transition in Cs and Rb occurs at identical critical populations of the *d* band.

Analysis of experimental data obtained on the compression of Cs by piezometric,[10,11] x-ray-diffraction,[12] and neutron-diffraction[13] methods, with allowance for a possible continuous change in the *s–d* nature of the conduction electrons,[9] has led to the suggestion[14] that Cs in the bcc phase should have a compressibility slightly higher than that of other alkali metals. However, a second, more careful study of the compression of Cs up to 2 GPa by a piston-displacement method failed to reliably detect anomalous compressibility of bcc Cs (Ref. 14).

This question can be resolved on the basis of direct measurements of the elastic properties of Cs, including the bulk modulus (compressibility) of the bcc phase, at high pressures by an ultrasonic method. There is particular interest in studying the properties of Cs before the bcc–fcc transition, in which case one might expect the appearance of soft modes in the phonon spectrum of the bcc Cs lattice.

The elastic constants of a Cs single crystal have been measured previously at atmospheric pressure, at $T = 4.2$, 63, and 78 K, by an ultrasonic method.[15] They have also been determined by coherent inelastic neutron scattering at 280 K (Ref. 16). We have carried out some preliminary high-pressure measurements of the velocity $v_l(p)$ of longitudinal ultrasonic wave, in Cs up to 5.0 GPa. These measurements demonstrated several anomalies in $v_l(p)$ (Ref. 17) and stimulated the detailed study which we are reporting here.

2. EXPERIMENTAL PROCEDURE AND RESULTS

In this paper we are reporting a study of the elastic properties of polycrystalline cesium at a temperature of 294 K and at pressures up to 2.5 GPa with a modified ultrasonic piezometer.[18] We also carried out experiments in a solid-state "flat-bottom-lens" chamber.[17] The transit times of the ultrasonic waves were determined through a visual superposition of signals, in a method refined for measurements with acoustic lines, at frequencies of 3 and 5 MHz. We used *x*- and *y*-cut quartz as piezoelectric transducers.

The Cs used in the measurements was 99.9% pure. Samples of this chemically aggressive substance, with its low melting point (301 K), were prepared and encapsu-

TABLE I. Elastic properties and propagation velocities of ultrasonic waves in cesium at $T=294$ K and $p=0$.

	Longitudinal wave		Transverse wave	
	Single crystal			
[hkl],[mnp]*	[100],[100]	[111],[111]	[100],[010]	[110],[1$\bar{1}$0]
c_{ij},	c_{11}	$(c_{11} + 2c_{12} + 4c_{44})/3$	c_{44}	$(c_{11} - c_{12})/2$
c_{ij}, GPa**	2.190	3.430	1.090	0.162
$v_{ij} = \sqrt{c_{ij}/\rho}$, км/c	1.076	1.347	0.759	0.293
	Polycrystalline sample			
v, km/s *** data of present study;	1.185		0.518	
Variable-length method	1.240 ± 0.040		-	
Piezometer measurements	1.220 ± 0.040		0.578 ± 0.090****	
Average value	1.230 ± 0.040		0.578 ± 0.090****	

*Wave propagation direction, polarization of wave

**extrapolation of data of Ref. 15 to $T=294$ K (the largest and smallest values are shown)

***Found by the method of Ref. 20 through the use of c_{ij}

****the average scatter from sample to sample is shown.

lated under a layer of thoroughly dried transformer oil. To avoid the formation of large-crystal blocks and to avoid recrystallization, the molten substance was poured from the opened ampule into a thin-walled aluminum mold and then rapidly cooled by immersion in liquid nitrogen. This was done just before an experiment. Test samples cut from the resulting ingot were placed in thin-walled aluminum cups or directly in the working volume of the ultrasonic piezometer.

The propagation velocities of longitudinal (v_{l0}) and transverse (v_{t0}) ultrasonic waves were determined at atmospheric pressure at $T=294$ K by a "variable-length" method, i.e., as a free test sample was compressed between two acoustic lines. In this case we have $v_0=\Delta l/\Delta t$. We also used an extrapolation to $p=0$ of measurements during the compression of cesium in the ultrasonic piezometer with unsealed pistons. In the measurements of the transverse-wave velocities, we observed a large scatter in the results from sample to sample. This scatter was due to the formation of crystalline blocks, partial recrystallization, and the pronounced anisotropy of the elastic properties of cesium: $c_{44}/c'=6.7$ and $v[100][010]/v[110][110]=2.6$, where c_{44} and $c'=(c_{11}-c_{12})/2$ are the shear elastic constants (Table I). We believe that the average results found from measurements on a large number (12) of independently prepared test samples give a reliable picture of the properties of polycrystalline cesium. The values shown for the velocities v_{l0} and v_{t0} in Table I were found by two methods. The results agree well with each other and also with estimates of the velocities v_{l0} and v_{t0} found for polycrystalline cesium found by an averaging, by the Peresada method,[20] of low-temperature data on Cs single crystals extrapolated to 294 K (Ref. 15).

The propagation velocities $v(p)$ of ultrasonic waves

and the compression of cesium in the initial pressure interval, 0–0.2 GPa, were determined with the help of an ultrasonic piezometer made of steel with pistons which were carefully fitted to the cylinder. These pistons were acoustic lines with a gap of 0.01 mm at a diameter of 18 mm. The Cs samples, 4–7 mm long, protected from oxidation by only a film of oil, were placed in a channel in the matrix without any seals. The stress applied to the pistons by a hydraulic press was measured with a standard DOSM-5 dynamometer. We carried out 15 experiments to determine $v_l(p)$ and 12 to determine $v_t(p)$ in this pressure interval.

An interlayer of a teflon film, 0.02 mm thick, between the test sample and the piston allowed us to raise the pressure to 1.1 GPa. Encapsulation of the samples in aluminum cups with a wall thickness ~ 1 mm and an end thickness ~ 0.6 mm, combined with the use of a compression plate of VK-6 tungsten carbide, extended the pressure range up to 2.5 GPa. In the experiments up to 1.1 and 2.5 GPa, the pressure was determined from the pressure under the plunger of the press and from the multiplication factor of the piezometer, with a correction for the enlargement of the matrix channel. In each of these ranges we carried out six measurements of $v_l(p)$ and $v_t(p)$. In the solid-state flat-bottom-lens chamber[17] we carried out seven determinations of $v_l(p)$ and $v_t(p)$. The results of all series of measurements were averaged; the results are shown in Fig. 1. The standard deviations for $v_l(p)$ are 1.2% and 1.5% at 0.2 and 2 GPa, respectively, and those for $v_t(p)$ are 3.1% at 2 GPa.

As the bcc–fcc phase transition is approached, a decrease in the amplitudes of the longitudinal and transverse waves transmitted through the sample is observed for the bcc Cs, while an increase in these amplitudes is observed at the bcc–fcc transition. The apparent reason for the de-
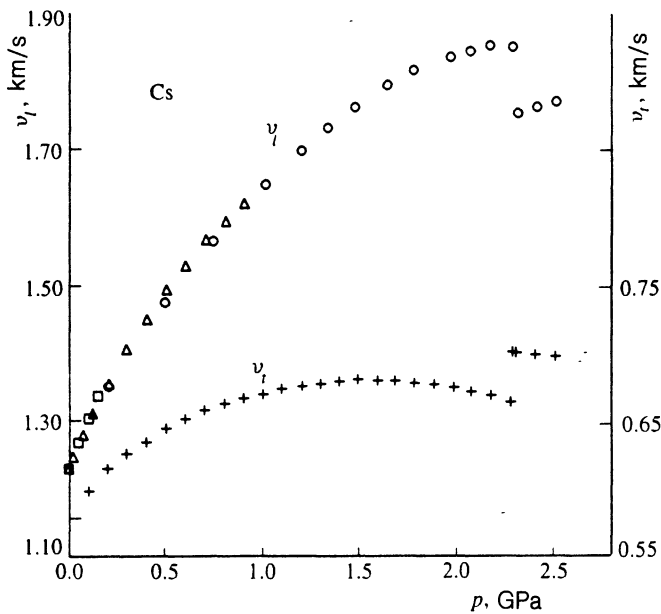
FIG. 1. Baric dependence of the propagation velocities of longitudinal (v_l) and transverse (v_t) ultrasonic waves in cesium. These are average experimental data (as explained in the text proper) on v_l. □—From 0 to 0.2 GPa; △—0 to 1.0; ○—0 to 2.5 GPa. Only some of the data under 1.0 GPa are shown, to avoid cluttering the figure.

crease in the signal amplitude is an increase in the phonon–phonon interaction, due to an increase in anharmonic effects in the pretransition region and (primarily) to an increase in the amplitude of the atomic vibrations. The increase in the amplitude at the transition may be due to both (on the one hand) the properties of the new phase and (on the other) crushing of crystallites in the sample and a change in the scattering by grains.

The bcc–fcc phase transition in cesium was detected from the abrupt changes in the length of the sample and in the transit time of the ultrasonic waves. These properties changed essentially instantaneously (in 0.1–0.3 s). The signal representing the shear vibrations disappeared completely in some of the experiments; on occasion, this signal appeared with a large time shift. In only three experiments was the shift of this signal traced continuously. At the transition the velocity of longitudinal waves decreases (5.3%), while that of transverse waves increases (5.6%).

These results imply an increase in the compressibility of cesium in the transition to the fcc phase. This increase has also been seen in neutron diffraction.[13]

The pressure of the bcc–fcc transition in Cs, which is frequently used as a reference point on the pressure scale, and the abrupt change in volume were determined in seven experiments on the ultrasonic piezometer, from the jumps on the $\Delta l(p)$ dependence. As the pressure is raised, the transition occurs at 2.28 ± 0.03 GPa; as the pressure is lowered, it occurs at 2.22 ± 0.02 GPa. The average phase-transition pressure which we found (2.25 ± 0.02 GPa) and the abrupt change in volume at the transition (0.70 $\pm 0.03\%$) are compared with the results of measurements by other investigators in Table II.

3. DETERMINATION OF ELASTIC CHARACTERISTICS AND DISCUSSION OF RESULTS

The experimental results on $v_l(p)$ and $v_t(p)$ were smoothed and used to calculate all the elastic characteristics of Cs over the pressure range 0–2.5 GPa. For adiabat-isotherm corrections at 294 K, the values of the specific heat, $c_p = 0.055$ cal/(g·deg), and its derivative, $\partial c_p/\partial T = 1.37 \cdot 10^{-4}$ cal/(g·deg^2), were determined from Ref. 23. The thermal expansion coefficient $\alpha = 3.0 \cdot 10^{-4}$ K^{-1} and its derivative $\partial\alpha/\partial T = 1.3 \cdot 10^{-6}$ K^{-2} were calculated on the basis of Ref. 24. The derivative of the isothermal bulk modulus, $\partial K_T/\partial T = -1.58 \cdot 10^{-5}$ GPa/K, was determined from Ref. 14. The corrections were assumed to be independent of the pressure and to be the same for the two Cs phases. The density of Cs at $p=0$ and 294 K, $\rho = 1.8893$ kg/m^3, was determined through a linear interpolation between the values $\rho = 1.9029$ kg/m^3 at 273 K and $\rho = 1.8860$ kg/m^3 at 299 K (Ref. 25). This result agrees well with the densities used in Refs. 10 and 14; it differs slightly from data from x-ray measurements[12] and from neutron-diffraction measurements[13] (the results of Refs. 12 and 13 do not agree with each other). The abrupt change in the density upon the bcc–fcc transition is taken to be 0.70% on the basis of our measurements.

In calculating the elastic properties of Cs from the ultrasonic data, we used the dependence of the compression of Cs on the pressure, $x(p) = V(p)/V_0$, up to 2.5 GPa, which is shown in Fig. 2 along with measurements by other investigators. The $x(p)$ dependence which we determined is in excellent agreement with the results of some recent

TABLE II. Parameters of the bcc–fcc phase transition in cesium.

T, K	p, GPa	V/V_0^*	$-\Delta(V/V_0)$,%	Year	Source
294	2.25 ± 0.02	0.6006	0.70 ± 0.03	1993	
298	2.25	0.602	0.6	1938	[21]
298	2.28	0.628	0.6	1948	[10]
298	2.26 ± 0.06	-	-	1962	[22]
295	2.24	0.589	0.6	1969	[11]
295	2.22	0.6024	0.63	1985	[14]

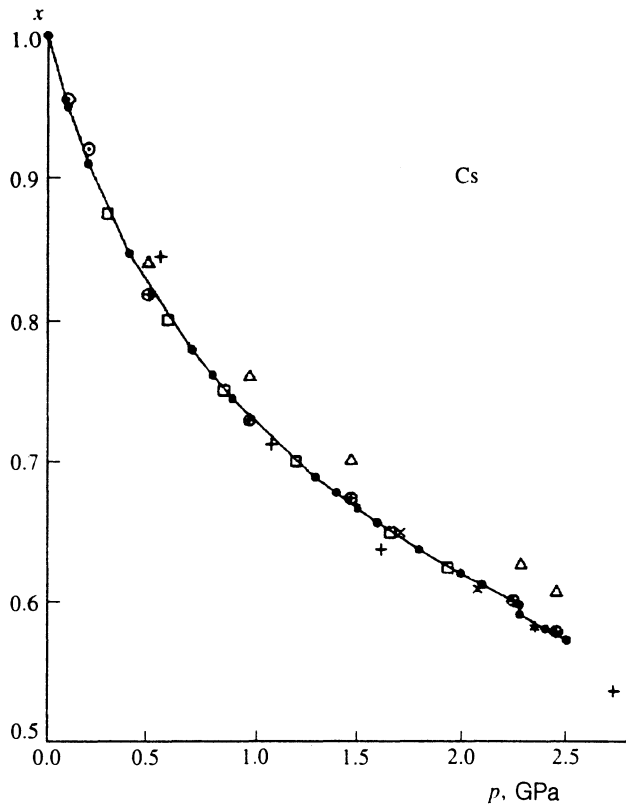*Value of V/V_0 at the time of the transition.

FIG. 2. The compression $x = V/V_0$ of cesium up to 2.5 GPa. Solid curve and filled circles—Data of the present study, on ultrasound; circles with dots—data of the present study, on isothermal compression; □—Ref. 14; △—Ref. 10; ⊕—Ref. 21; +—Ref. 13; ×—Ref. 26; *—Ref. 12.

piezometric measurements[14] and also some x-ray diffraction[26] and neutron-diffraction[13] studies. These results also agree well with the early measurements by Bridgman, in Ref. 21, while Bridgman's more recent data[10] (better data in his opinion) deviate in the direction of smaller values of x. The values of the compression of Cs which we determined directly from the displacement of the piezometer piston, $\Delta l(p)$, agree with the $x(p)$ dependence from the ultrasonic measurements.

The results on $x(p)$ for Cs are compared with data for other alkali metals[10,21,27,28] in Fig. 3, as functions of the reduced pressure $p/K_{T,0}$. To construct the reduced pressure for the case of cesium we used our value $K_{T,0} = 1.81$ GPa and the values 11.5, 6.13, 3.09, and 2.38 GPa for Li, Na, K, and Rb, respectively, found from ultrasonic measurements on single crystals.[29-32] Adiabat-isotherm corrections and a temperature correction were incorporated on the basis of Ref. 28. We see in Fig. 3 that the compression of all the alkali metals, including cesium, can be described by a common plot up to $p/K_{T,0} = 0.6$–0.8. At $p/_{T,0} > 0.8$, cesium exhibits high compressibility: The $x(p/K_{T,0})$ curve for cesium runs below the points for the other alkali metals. It was noted in Ref. 14 that the compression of Cs at 2.2 GPa ($p/K_{T,0} = 1.3$) is 5% greater than that for Na, K, and Rb.

That there are no anomalies in the values of the initial

compressibility κ_0 of cesium and in the baric derivative of the bulk modulus $K'_{T,0}$ at $p = 0$ is clear from Fig. 4, where these properties are plotted against the molar volume for all the alkali metals. The value $K'_{T,0} = 3.4$ calculated from the adiabatic elastic modulus which we found, $K'_{S,0} = 3.7$, is slightly smaller than the piezometric values 3.56 (Ref. 33) and 3.87 (Ref. 14), but it lies in the interval $K'_{T,0} = 3.5$–4.2 characteristic of alkali metals, within the errors.

The elastic characteristics which we found for cesium as a function of the pressure up to 2.5 GPa are shown in Table III. We see a substantial increase in the elastic characteristics with the pressure. For example, when the pressure reaches the level of the initial bulk modulus of Cs, $p = 1.8$ GPa, the bulk modulus K_S increases by a factor of 4, while the Young's modulus E_S and the shear modulus G increase by a factor of 2.2. At the point of the bcc–fcc transition, the increase in the moduli slows down, and $\partial G/\partial p$ goes negative. The onset of peaks on the plots of the elastic characteristics and also of the Debye temperature Θ_D correlates with the peak on the melting curve of bcc Cs at 2.0 GPa. The substantial changes in the elastic characteristics are due to a significant decrease in the interatomic distances during the compression of cesium; this decrease reaches 15% at 2.0 GPa.

Since the elastic characteristics are second derivatives of the free energy with respect to the corresponding strains, features of the change in the energy spectrum of Cs in compression can be found by analyzing the behavior of the elastic moduli as a function of the change in interatomic distances, $y = r/r_0 = a/a_0 = x^{1/3}$.

Figure 5 shows curves of $K_T(y)$ and $K'_T(y)$ found from our experiments and also some curves calculated from a simple model of an alkali metal in which the binding energy per atom, E_c, is represented as the sum of the energy of a low state of valence electrons, $E_0 = \widetilde{A}/r^3 - \widetilde{C}/r$, and the average Fermi kinetic energy $E_F = \widetilde{B}/r^2$:

$$E_c = A/x + B/x^{2/3} - C/x^{1/3}, \quad x = V/V_0. \tag{1}$$

Equation (1) is written under the assumption that the electron wave functions near the boundaries of the atomic polyhedra do not differ greatly from those for free electrons and that the average effective masses of the electrons are independent of the atomic volume near the equilibrium volume. As in Ref. 30, we determined the parameter values $A = 3.45$, $B = 0.66$, and $C = 11.67$, in units of 10^{-12} erg/atom, for Cs from the binding energy per atom, the equilibrium condition $p = 0$, and K_T at $T = 0$, found by extrapolating $K_T(T)$ to $T = 0$ on the basis of Ref. 14.

Systematic differentiation of (1) and a transformation to $y = x^{1/3}$ lead to

$$K_T(y) = (18A/y^6 + 10B/y^5 - 4C/y^4)/9V_0 \tag{2}$$

$$K'_T(y) = \partial K_T(y)/\partial p$$

$$= (108A/y^6 + 50B/y^5 - 16C/y^4)/$$

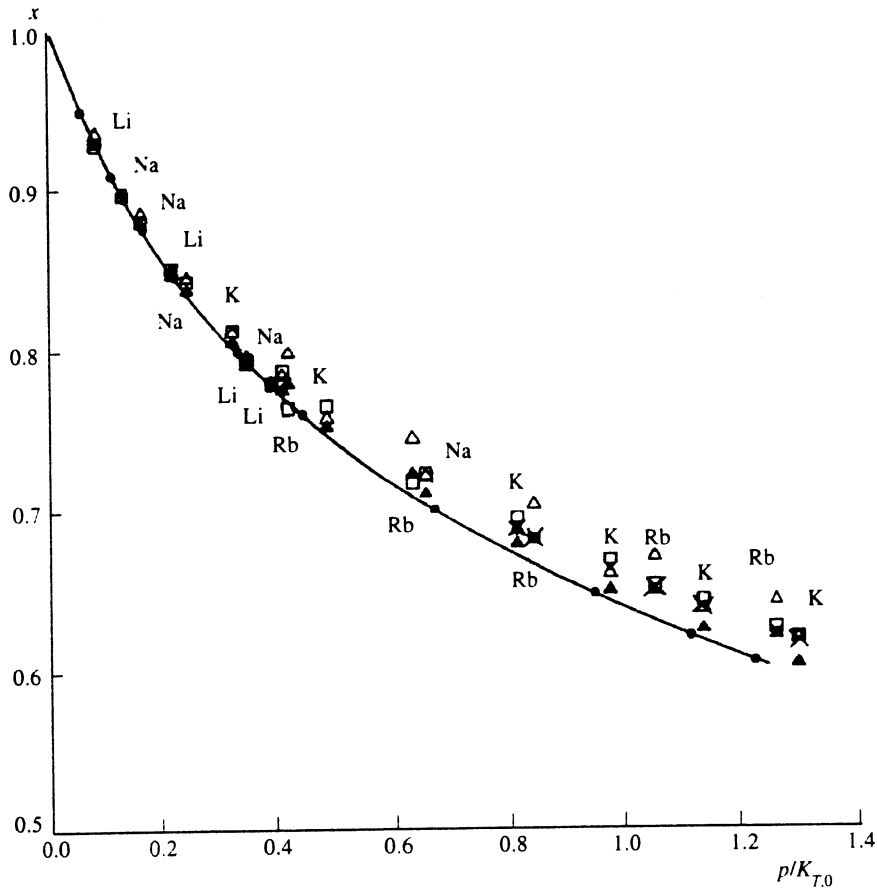$$3(18A/y^6 + 10B/y^5 - 4C/y^4). \tag{3}$$

FIG. 3. Compression of alkali metals versus the reduced pressure. Solid curve and ●—Cs, data of present study; △—Ref. 10; □—Ref. 21; ▲—Ref. 27; ×—Ref. 28.
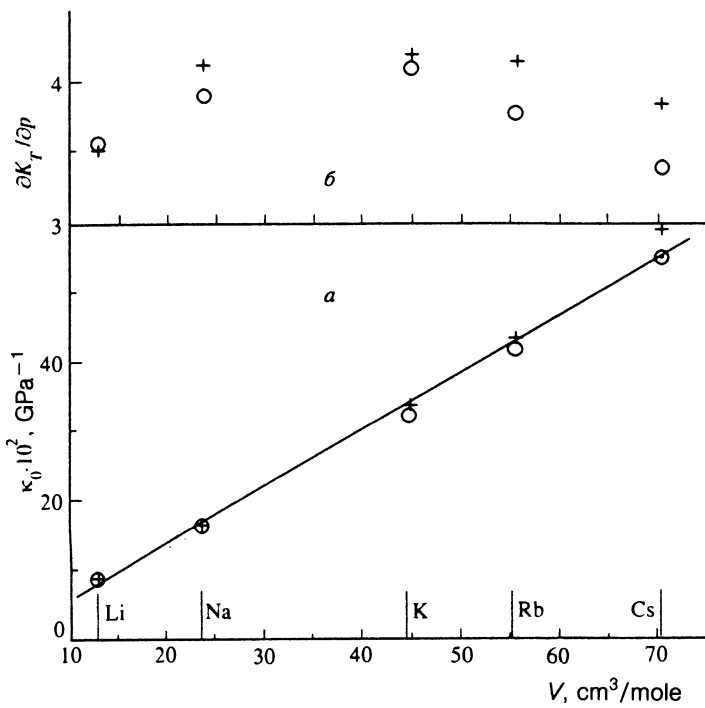

FIG. 4. Initial compressibility $\varkappa_0$ and $\partial K_T/\partial p$ at $p=0$ for alkali metals. ○—Ultrasonic data on Li (Ref. 29), Na (Ref. 28), K (Ref. 31), and Rb (Ref. 32); ⊙—Cs, data of present study; plus signs—piezometric data on Li and Cs (Ref. 14) and Na, K, and Rb (Ref. 28).

TABLE III. Elastic properties of cesium at pressures up to 2.5 GPa.

p, GPa	x	K_S, GPa	G, GPa	E_S, GPa	σ^*	θ_D
			bcc Cs			
0.0	1.0000	2.016	0.631	1.714	0.358	39.64
0.2	0.9106	2.776	0.774	2.126	0.372	43.31
0.4	0.8481	3.505	0.898	2.482	0.382	46.16
0.6	0.8003	4.189	1.002	2.784	0.389	48.33
0.8	0.7618	4.847	1.090	3.042	0.395	50.04
1.0	0.7297	5.503	1.166	3.266	0.401	51.41
1.2	0.7023	6.159	1.231	3.462	0.406	52.54
1.4	0.6786	6.809	1.287	3.633	0.411	53.45
1.6	0.6577	7.429	1.330	3.765	0.416	54.09
1.8	0.6390	7.996	1.363	3.869	0.419	54.52
2.0	0.6220	8.490	1.386	3.943	0.423	54.75
2.2	0.6062	8.851	1.395	3.975	0.425	54.71
2.28	0.6002	8.939	1.392	3.969	0.426	54.57
			fcc Cs			
2.28	0.5932	7.706	1.570	4.409	0.405	57.67
2.30	0.5903	7.752	1.573	4.419	0.405	57.70
2.40	0.5763	7.968	1.589	4.469	0.407	57.87
2.50	0.5628	8.186	1.604	4.518	0.408	58.03

*here σ is the absorption coefficient.

A comparison of $K_T^{\exp}(y)$ and $K_T^{\text{theor}}(y)$ shows that these curves run parallel to each other up to $y=0.88$ ($p=1.4$ GPa; Fig. 5). At high pressures, $K_T^{\exp}(y)$ deviates towards smaller values of K_T, causing the cesium to exhibit compression values at $p/K_{T,0}>0.8$ (Fig. 2) which are large in comparison with those of other alkali metals. The baric derivative $K_T'^{\exp}(y)$, which is equal to 3.4 at $p=0$, falls off slightly with the pressure. At $y=0.88$ it has a slope change and then falls off rapidly to values of 0.8–0.9 near the beginning of the bcc–fcc phase transition. The theoretical value $K_T'^{\text{theor}}(y)$, on the other hand, which is equal to 3.31 at $p=0$, falls off monotonically with the pressure.

The anomalies found in the compressibility of Cs at $y<0.88$ ($p>1.4$ GPa), i.e., the increase in the compression, the deviation of $K_T^{\exp}(y)$ from the theoretical curve, the sharp slope change, and the decrease in $K_T'^{\exp}(y)$, cannot be described on the basis of this simple model of an alkali metal. For $y<0.88$ it appears that either an additional negative contribution to the lattice energy and the bulk modulus arises, or the parameters A, B, and C in Eqs. (2) and (3) become independent of the compression. This would correspond to a change in the population of the s band with the pressure, i.e., to an s–d transition. In the case of anomalous $K_T(p)$ and $K_T'(p)$ curves, equations of the Murnagan and Birch type are unsuitable, and their application to Cs results in an incorrect interpretation of the measurements.

Analysis of the baric dependence of the shear elastic characteristics of cesium, $v_t(p)$ and $G(p)$, shows that these characteristics, like the bulk modulus, exhibit anomalies only at high pressures. The baric derivatives $\partial G/\partial p$ for Cs

at $p=0$ which we found experimentally and by averaging the quantities $\partial c_{44}/\partial p$ and $\partial c'/\partial p$, taken from pseudopotential calculations,[34,35] agree well (Table IV). This agreement leads us to conclude that there are no structural features in $G(p)$ near $p=0$.

Let us compare (on the one hand) the change in the shear modulus of Cs with decreasing interatomic distance and (on the other) the change in the contribution of the electrostatic energy E^e to the shear elastic constants:

$$c_{ij}=\partial^2(E^e+E^b)/\partial u_{ij}\partial u_{ij}=c_{ij}^e+c_{ij}^b, \tag{4}$$

where c_{ij}^b is the contribution of the "one-particle" band energy E^b, c_{ij}^e is the contribution of the electrostatic energy, and u_{ij} are strains. For alkali metals, whose Fermi surface is approximately spherical, lies in the Brillouin zone, and varies only slightly in the course of purely shear deformations, the shear elastic constants are dominated by the energy of the long-range electrostatic interaction E^e. For bcc alkali metals this contribution is[36]

$$c_{44}^e=0.7423Z_0 e^2/a^4; \quad c'^{\,e}=0.0997Z_0 e^2/a^4, \tag{5}$$

where e is the charge of an electron, a is the lattice constant, and Z_0 is the electron density at the boundary of the Wigner–Seitz cell or the valence. We have $Z_0=1$ when this density is equal to the density of the charge distributed uniformly over volume: e/Ω_0, where Ω_0 is the volume per atom.

The elastic constants calculated for Cs from (5) agree with the results of measurements[15] at $T=4.2$ K and $p=0$ to within 10–12%. This circumstance demonstrates the dominant role of the electrostatic component of the elastic constants. Taking an average of (5) as in (20), we find the "electrostatic shear modulus" for polycrystalline samples:

$$G^e=0.3324Z^2 e^2/a^4. \tag{6}$$

This quantity, like c_{44} and c', should vary in proportion to a^{-4}. Studies of Na and K at pressures up to 1.0 GPa have revealed the logarithmic derivatives $\partial \ln c_{44}/\partial \ln a$ and $\partial \ln c'/\partial \ln a$ for these metals. The results turn out to be -7.2 and -7.2 for Na (Ref. 28) and -7.8 and -8.1 for K (Ref. 31). In other words, these values are essentially equal to each other, in agreement with (5), but instead of being equal to -4 they are close to -8. This result suggests that Z varies according to $Z=Z_0(a_0/a)^2$ in the course of the compression.[31]

The value which we found for $G=f(a/a_0)$ for Cs, and which is shown in logarithmic coordinates in Fig. 6, passes between $f(a^{-4})$ and $f(a^{-8})$ and is close to $f(a^{-6})$ up to $y=0.88$. Further on, it deviates towards smaller values of $\ln G$. Consequently, again in the case of Cs the electron density Z depends on the compression, but the dependence is not as strong as proposed in Ref. 31.

The logarithmic derivative of the shear modulus, $\partial \ln G/\partial \ln a$, which is equal to -6.7 at $p=0$, falls off in absolute value to -4 with the pressure. It changes slope at $y=0.88$ and then rapidly drops to zero at the point of the bcc–fcc transition (Fig. 6). Correspondingly, the derivative of the electron density Z with respect to the lattice constant at the boundary of the Wigner–Seitz cell,
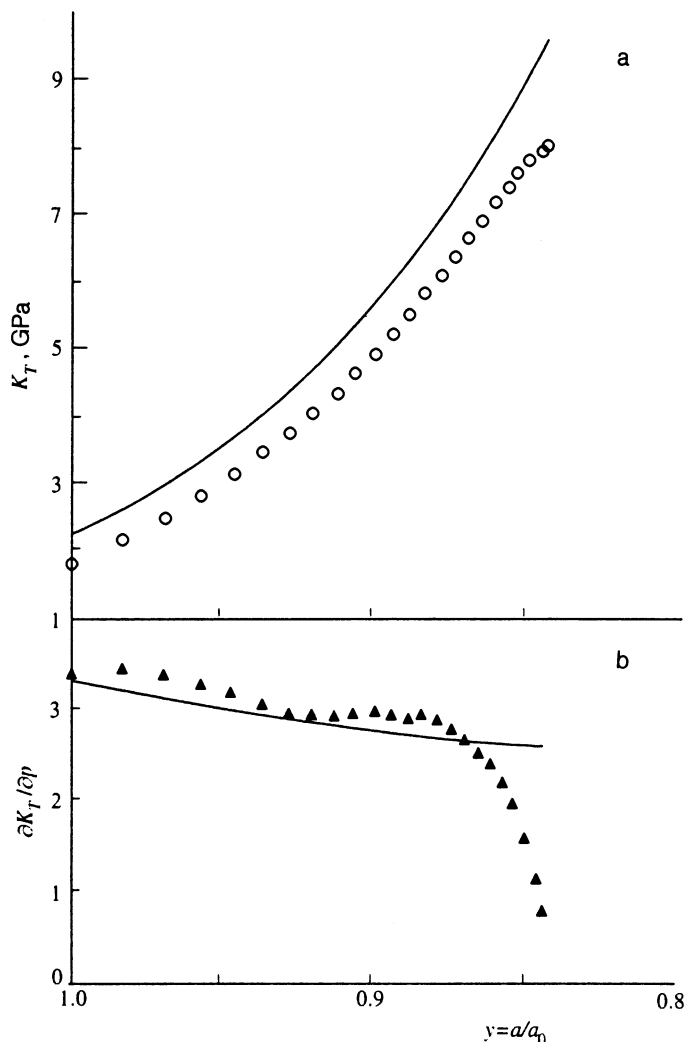
FIG. 5. Experimental and theoretical results on the bulk modulus of Cs (a) and its baric derivative (b) versus the compression. Solid curve—Theoretical; points—experiments of the present study.

$$\partial \ln Z/\partial \ln a = (\partial \ln G/\partial \ln a - 4)/2, \tag{7}$$

goes from negative values (corresponding to an increase in the electron density in compression) to positive values (corresponding to a decrease in this density) at the point $y=0.88$. The decrease in the electron density at the cell boundary causes the anomalies which we observed on the plots of the elastic characteristics of Cs as a function of the pressure at $y<0.88$. The apparent reason for the decrease in the electron density is a transition of electrons from an s state into a more-localized $5d$ band.

Some theoretical calculations carried out on the Cs band structure by the self-consistent $X\alpha$ method showed that an s–d transition can occur in Cs during compression

TABLE IV. Baric derivative of the shear modulus of cesium at $p=0$.

Source	$\partial G/\partial p$	T, K
present experiments	0.76	294
Calculations of Ref. 35*	0.68	294
Calculations of	0.61	0
Ref. 36 sh GT	0.47	0

beginning at $p=0$ (Refs. 5 and 6). Some more recent calculations carried out by the LMTO–ASA pseudopotential method, on the basis of one-electron theory, showed that the change in the s–d nature of the conduction electrons begins not at $p=0$ but only when the volume has decreased to $x=0.82$, at which point the Van Hove singularity associated with the X_1 symmetry point of the free $5d$ band begins to cross the Fermi level.[7]

It was also mentioned in Ref. 7 that the energy difference between the bcc and fcc structures of Cs disappears later, at a compression $x=0.7$. A delay of this sort is characteristic of transitions caused by changes in electronic states. Our studies of Cs support the results of the latter calculations. We observed the onset of anomalies in the elastic properties of Cs due to an s–d transition not at $p=0$ but at $x=0.68$, and the bcc–fcc transition occurred after a delay, at $x=0.60$.

Before the bcc–fcc transition, the derivative $\partial \ln G/\partial \ln a$ passes through a value of -1 at a compression $x=0.618$, and the Grüneisen parameter

$$\gamma_t = -1/6\partial \ln G/\partial \ln a - 1/6 \tag{8}$$

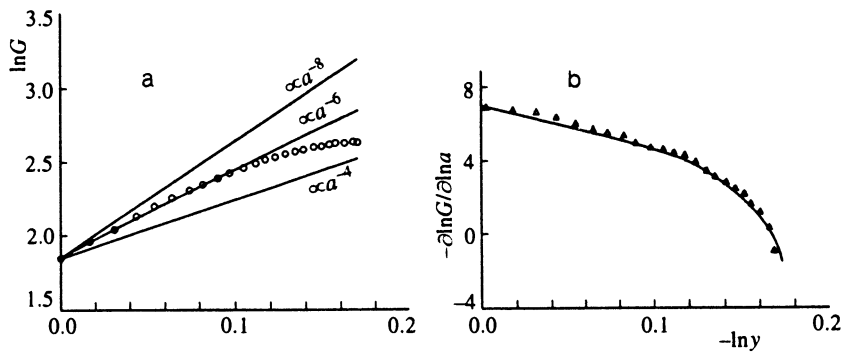goes negative. This result indicates that a soft shear mode

FIG. 6. The shear modulus of Cs (a) and its derivative (b) versus the compression. Solid lines—Theoretical; points—results of the present experiments.

appears in the low-frequency part of the Cs phonon spectrum. Our measurements on polycrystalline samples cannot tell us which mode, TA_1 or TA_2, becomes soft. At best we can suggest that, on the basis of the mechanism for the restructuring of the bcc–fcc lattices—a uniform shift in the (110) plane in the [110] direction[37]—that this mode is the TA_1 mode, which is associated with the elastic constant which is smallest in magnitude, $c' = (c_{11} - c_{12})/2$ (Ref. 15; see also Table I of the present paper). The conclusion that no softening effects occur on the baric dependence of the shear elastic constants of bcc Cs before the bcc–fcc transition—a conclusion reached in a theoretical paper[38]—thus does not find support here.

The bcc–fcc transition in Cs at high pressures should be classified as a martensitic transition, characterized by a cooperative displacement of atoms and by a rapid occurrence, as we saw in the rapid shift of the ultrasonic signal on an oscilloscope screen. In the course of the bcc–fcc transition the shear modulus of Cs increases by 12.8%, because of an increase in the coordination number and a transition to a denser structure. On the other hand, the denser fcc phase of Cs has a greater compressibility, and according to the estimates of Ref. 14 the bulk modulus should decrease 10% at the transition. Our measurements showed that this decrease is 13.8%. The decrease in K_T can be attributed to an increase in the shortest distance between nearest neighbors upon the transition to the more closely packed structure.

We sincerely thank A. F. Barabanov for a discussion of this study and V. K. Luĭkh for the excellent preparation of the apparatus and for assistance in the experiments.

[1] Yu. E. Tonkov, Phase Diagrams of Elements at High Pressures [in Russian] (Nauka, Moscow, 1979), p. 192.

[2] K. Takemura and K. Syassen, Phys. Rev. B 32, 2213 (1985).

[3] J. Yamashita and S. Asano, J. Phys. Soc. Jpn. 29, 264 (1970).

[4] F. W. Averill, Phys. Rev. B 4, 3315 (1971).

[5] A. K. McMahan, Phys. Rev. B 17, 1521 (1978).

[6] D. Glotsel and A. K. McMahan, Phys. Rev. B 20, 3210 (1979).

[7] H. L. Skriver, Phys. Rev. B 31, 1909 (1985).

[8] T. M. Eremenko and E. V. Zarochentsev, Solid State Commun. 30, 785 (1979).

[9] H. Tups et al., Phys. Rev. Lett. 49, 1776 (1982).

[10] P. W. Bridgman, Proc. Am. Acad. Arts Sci. 76, 71 (1948).

[11] M. S. Anderson et al., J. Phys. Chem. Solids 30, 1587 (1969).

[12] C. E. Weir et al., J. Chem. Phys. 54, 2768 (1971).

[13] D. B. McWhan et al., J. Phys. F 4, L69 (1974).

[14] M. S. Anderson and C. A. Swenson, Phys. Rev. B 31, 668 (1985).

[15] F. J. Kollarits and J. Trivisonno, J. Phys. Chem. Solids 29, 2133 (1968).

[16] J. Mizuki and C. Stassis, Phys. Rev. B 34, 5890 (1986).

[17] F. F. Voronov et al., High Pressure Res. 6, 213 (1991).

[18] F. F. Voronov and O. V. Stal'gorova, Prib. Tekh. Eksp., No. 5, 207 (1966).

[19] E. P. Papadakis, Rev. Sci. Instrum. 47, 805 (1976).

[20] G. I. Peresada, Phys. Status Solidi A 4, K23 (1971).

[21] P. W. Bridgman, Proc. Am. Acad. Arts Sci. 72, 207 (1938).

[22] G. Kennedy and P. N. LaMori, J. Geophys. Res. 67, 851 (1962).

[23] Properties of the Elements Part I [in Russian], ed. by G. V. Samsonov (Metallurgiya, Moscow, 1976), pp. 67–68.

[24] D. L. Martin, Phys. Rev. A 1, 150 (1965).

[25] L. Hackspill, C. R. Acad. Sci. 152, 259 (1911).

[26] H. T. Hall et al., Science 146, 1297 (1964).

[27] S. N. Vaidya, J. Phys. Chem. Solids 32, 2545 (1971).

[28] M. S. Anderson and C. A. Swenson, Phys. Rev. B 28, 5395 (1983).

[29] R. A. Felice et al., Phys. Rev. B 16, 5173 (1977).

[30] W. Daniels, Phys. Rev. 119, 1246 (1960).

[31] P. A. Smith and C. S. Smith, J. Phys. Chem. Solids 26, 279 (1965).

[32] L. A. Pauel, U. S. Office of Naval Research Rep. N AD 670520 (cited in Ref. 27).

[33] I. N. Makarenko et al., Liquid Metals, ed. by R. Evans and D. A. Greenwood (I.O.P., Bristol, 1977), p. 79.

[34] V. G. Vaks et al., J. Phys. F 8, 725 (1978).

[35] E. V. Zarochentsev et al., Fiz. Nizk. Temp. 3, 209 (1977) [Sov. J. Low Temp. Phys 3, 100 (1977)].

[36] K. Fuchs, Proc. Roy. Soc. A 153, 622 (1936).

[37] C. Zener, Phys. Rev. 71, 846 (1947).

[38] V. G. Vaks et al., J. Phys. Cond. Matt. 3, 1409 (1991).

Translated by D. Parsons